R. & M. No. 2851
(12,173, 12,476, 14,222)
A.R.C. Technical Report

MINISTRY OF SUPPLY

AERONAUTICAL RESEARCH COUNCIL
REPORTS AND MEMORANDA

Tunnel-Wall Effect on an Aerofoil at Subsonic Speeds

By

A. Thom and Laura Klanfer

LONDON: HER MAJESTY'S STATIONERY OFFICE
1957
PRICE 6s 0d NET

Tunnel-Wall Effect on an Aerofoil at Subsonic Speeds

By

A. THOM AND LAURA KLANFER

Reports and Memoranda No. 2851

August, 1951

Summary.—This is a detailed study of the effect of the presence of walls on the flow past a symmetrical aerofoil at zero incidence. The low-speed case is considered first, followed by solutions at a Mach number of 0·7. The methods used are essentially arithmetical, but a new approach is used for the compressible case. The manner in which the walls affect the pressure distribution is clearly shown.

1. *Introduction.*—In an earlier paper[1] a study was made of the compressible flow past a cusped body in a channel. The present paper deals with the corresponding case for an aerofoil. The first few sections describe in detail the arithmetical solution of the incompressible flow past an aerofoil between parallel walls by a superposition method which is capable of dealing with a variety of problems. This is followed by a solution at a Mach number of 0·70. As this solution was made using a grid of 10 squares to the chord some doubt existed as to its accuracy. Accordingly the work was repeated with 20 squares to the chord.

1.1. In order to make a detailed study by arithmetical methods of the compressible flow past a body between walls it is desirable to have a grid on which the solution can be conveniently worked. This grid is the orthogonal net given by the incompressible solution. As the object of the investigation is to find the effect of the presence of the walls we really require two grids or nets, namely the free-stream case and the walled or bounded case. In order to keep the effect of the neglected terms as small as possible it was thought advisable to keep the two nets in the vicinity of the body as similar as possible. Consider, for example, Fig. 1a where the depth of the net is two squares and the quadrant of the body abcs is an integral number of squares. In the free-stream case (Fig. 1a) the equipotential $\phi = 3$ springs from the stagnation point s. If now parallel walls are superimposed having a total spacing at infinity of 4 squares (2 to the half width) the velocity past the body will rise and the equipotential spacing will decrease. The nets will be no longer alike, especially in the neighbourhood of the stagnation point where the equipotential $\phi = 3$ will no longer spring from s but from s_1 (Fig. 1c). To return it to s we must increase the wall spacing or decrease the size of the body.

Having returned the line $\phi = 3$ to s it does not follow that the foot of the intermediate equipotentials at b and c have come back exactly to the same places as in the unbounded case. It is found that in fact ab shortens slightly, which means that walls tend to produce a greater rise in velocity (or blockage effect) at the central portions of an aerofoil than towards the ends (*see* Ref. 1). It is evident that the mean blockage effect over the whole aerofoil is approximately the percentage decrease in the size of the aerofoil necessary to return the streamline $\phi = 3$ to s, and the movement of b and c is then a measure of the distortion of the flow produced by the wall.

In so far as this distortion can be neglected the method of this paper gives the grid constants directly without laborious repetition. The movement of the intermediate points b and c can then be calculated and allowed for in a second and, if necessary, a third approximation.

It will be evident from the above that we do not set out to solve the problem for a given ratio of channel width to chord. The exact value we have used is only found after the solution is complete.

2. *Theory of the Method for Incompressible Flow.*—Fig. 1a shows the open field grid in the $z = x + iy$ field and Fig. 1b the grid for the bounded field. Figs. 1d and 1e show these grids in the $w = \phi + i\psi$ fields. Let the relation between 1a and 1d (unbounded case) be $z_O = f_O(w)$ and that between 1b and 1e (bounded case) be $z_B = f_B(w)$.

Then

$$\left.\begin{aligned} \log\frac{1}{q_O} + i\theta_O &= \log\frac{dz_O}{dw} = f'_O(w) \\ \log\frac{1}{q_B} + i\theta_B &= \log\frac{dz_B}{dw} = f'_B(w) \end{aligned}\right\} \quad .. \quad .. \quad .. \quad .. \quad (1)$$

or, subtracting

$$\begin{aligned} \log\frac{q_O}{q_B} + i(\theta_B - \theta_O) &= f'_B(w) - f'_O(w) \\ &= \text{say } f'(w) \; . \end{aligned} \quad .. \quad .. \quad .. \quad .. \quad .. \quad (2)$$

Hence our problem is solved when we have found $f'(w)$ since $f'(w)$ added to the open field gives the bounded field. So we start by calculating the value of θ at d, e, f, g, etc., in the open field. The corresponding values of θ in the bounded field are zero, or if the walls are not straight and parallel the θ values are known. Neglect in the first place the movements of b and c. In other words take $(\theta_B - \theta_O)$ zero everywhere along the lower boundary. Thus we have all the boundary values and can 'square' the field directly. (Ref. 7.)

Now since all the networks are conformal

$$\frac{\partial}{\partial\phi}\log\frac{q_O}{q_B} = \frac{\partial}{\partial\psi}(\theta_B - \theta_O) \; . \quad .. \quad .. \quad .. \quad .. \quad .. \quad .. \quad (3)$$

This gives the ratio q_B/q_O of the bounded to the unbounded velocity in the form

$$\log\frac{q_O}{q_B} = \int \frac{\partial(\theta_B - \theta_O)\, d\phi}{\partial\psi}$$

and

$$\log\frac{q_O}{q_B} = \int \frac{\partial(\theta_O - \theta_B)\, d\psi}{\partial\phi} \quad .. \quad .. \quad .. \quad .. \quad .. \quad .. \quad (4)$$

where, as before, the subscript O refers to the open field and B to the bounded. The integration can be started at any point where the velocity is known, *e.g.*, in the undisturbed stream.

2.1. *Second Approximation.*—If s is measured along a streamline, $q = d\phi/ds$, so that $ds = (1/q)\, d\phi$, $dx = (1/q)\cos\theta\, d\phi$ and $dy = (1/q)\sin\theta\, d\phi$. Thus from the first approximation we can by integration find values of x and y at any point. At present we are only really interested in the amount by which the points on the surface like b and c have moved so as to find the true value of $\theta_B - \theta_O$ at these points. It is not advisable to try to find x or y directly because, in the integrals, $1/q$ becomes infinite at stagnation points. The main virtue of the present solution is in fact that this infinity at the stagnation points can be avoided by using the differences from the known free-stream solution. We have

$$\left.\begin{aligned} x_O &= \int\frac{1}{q_O}\cos\theta_O\, d\phi \\ x_B &= \int\frac{1}{q_B}\cos\theta_B\, d\phi \end{aligned}\right\} \; .. \quad .. \quad .. \quad .. \quad .. \quad (5)$$

Neglecting the difference between $\cos\theta_O$ and $\cos\theta_B$ we have

$$\delta x = x_B - x_O = \int\left(\frac{1}{q_B} - \frac{1}{q_O}\right)\cos\theta_O\, d\phi \; . \quad .. \quad .. \quad .. \quad .. \quad (6)$$

If we integrate from one end of the body (or aerofoil) to the other we obtain the total reduction in the chord, *i.e.*, the amount by which we imagine the aerofoil reduced in size in order to obtain as nearly similar grids as possible in the open and closed fields (*see* section 1.1). Calling this reduction δc we have

$$r = c_O/c_B = c_O/(c_O - \delta c) \qquad (7)$$

as the ratio of the chords. Having then obtained δx for any point on the surface of the body, and knowing x_O we find x_B from $x_B = x_O + \delta x$. Then scaling this up in the ratio r we obtain

$$\Delta x = r x_B - x_O . \qquad (8)$$

Knowing the geometry of the body we have $d\theta/dx$ and so

$$\theta_B - \theta_O = \Delta\theta = \Delta x \, d\theta/dx . \qquad (9)$$

The values thus calculated are the new boundary values of $\theta_B - \theta_O$ along the lower boundary ($\psi = 0$) of the grid.

There is no need to begin to square the θ field again completely. All we need do is to start a new θ field with the above values of θ written at the appropriate points on the lower boundary and with the upper boundary everywhere zero. Having squared this field it is simply complementary to the original θ field, which remains unaltered throughout. Thus we can proceed to obtain a second set of values of $\Delta\theta$.

It will be seen that throughout the whole solution we operate on the difference between the open and bounded fields and so the accuracy of the result is increased.

3. *Application of the Method for the Incompressible Case.*—The method outlined in section 2 was applied to a symmetrical aerofoil. The aerofoil used is one of the series developed by Piercy, Piper and Preston[4,5] by transformation from a hyperbola. The trailing-edge angle was taken as 0·3735 radians. This makes the maximum thickness $t/c = 14{\cdot}34$ per cent at 34 per cent of the chord.

With $\phi = \pm 2$ at the leading edge and trailing edge respectively the co-ordinates x, y of any point on the grid are given by

$$x = \frac{1 + \cosh u \, \cos v}{(\cosh u + \cos v)^2}, \qquad y = \frac{\sinh u \, \sin v}{(\cosh u + \cos v)^2} \qquad (10)$$

where u and v are obtained* from

$$\alpha = \sqrt{\{(\phi + 2)^2 + \psi^2\}}, \qquad \beta = \sqrt{\{(\phi - 2)^2 + \psi^2\}}$$

$$\cosh^2 \frac{u}{\omega} = \frac{\alpha + \beta + 4}{2\alpha} \qquad \sin^2 \frac{v - \sigma\pi}{\omega} = \frac{\alpha + \beta - 4}{2\alpha}$$

$$\omega = 2(1 - \sigma), \qquad 2\pi\sigma = \tau = \text{trailing-edge angle.}$$

The velocity vector is given by

$$q = \frac{1}{2\omega^3} \alpha\sqrt{\beta} \, \frac{(\cosh v + \cos v)^{3/2}}{(\cosh u - \cos v)^{1/2}} \qquad (11)$$

$$\theta = \frac{\pi}{2} - \tfrac{1}{2} \tan^{-1} \frac{\psi}{\phi - 2} - \tan^{-1} \frac{\psi}{\phi + 2} + \tan^{-1} \gamma \qquad (12)$$

where

$$\gamma = \frac{\sin v}{\sinh u} \, \frac{1 - \sinh^2 u + \cosh u \, \cos v}{\cos^2 v - 2 - \cos v \, \cosh u} .$$

---

* u and v are *not* velocity components in the physical plane.

The velocity has been multiplied by $2\omega^2$ to make it equal to unity at infinity.

3.1. The co-ordinates of the aerofoil are given in Table 1 and Table 4. Using the above formulae values for θ_O, the direction of the velocity vectors in the unbounded field, were calculated along $\psi = 4$. But here $\theta_B = 0$, so the upper boundary of the $(\theta_B - \theta_O)$ field was known. On the lower boundary $(\theta_B - \theta_O)$ was assumed zero in the first approximation. This field was squared (*see e.g.*, Ref. 7) and using equation (4) values of $\log q_O/q_B$ were obtained. Then new boundary values on the lower boundary were calculated according to equations (6) to (9). It was found that the movements $\Delta\theta$ were small, as will be seen by the values in Table 2.

TABLE 1

Co-ordinates of Aerofoil Profile. ($c = 0{\cdot}50438$)

ϕ	x	y
−2	0	0
−1·6	0·06043	0·01068
−1·2	0·11509	0·01901
−0·8	0·16745	0·02567
−0·4	0·21828	0·03077
0	0·26793	0·03426
0·4	0·31663	0·03600
0·8	0·36453	0·03570
1·2	0·41174	0·03276
1·4	0·43511	0·02990
1·6	0·45834	0·02565
1·8	0·48142	0·01901
2	0·50438	0

TABLE 2

ϕ	$\Delta\theta$ (1st round)	$\Delta\theta$ (2nd round)
−2	0	0
−1·6	−0·00003	−0·00003
−1·2	−0·00004	−0·00004
−0·8	−0·00005	−0·00004
−0·4	−0·00004	−0·00004
0	−0·00003	−0·00003
0·4	−0·00003	−0·00002
0·8	−0·00001	0
1·2	+0·00002	+0·00002
1·4	+0·00002	+0·00002
1·6	+0·00008	+0·00004
1·8	+0·00009	+0·00004
2	0	0

Evidently there is no need to make a further repetition. Differentiating across and integrating along $\psi = 0$ in the $\Delta\theta$ field incremental boundary values of $\log q_O/q_B$ were obtained and the field squared. These values added to the values found from the first approximation give the final values of $\log q_O/q_B$.

The velocities in the unbounded case were found by calculating values of $\log q_O$ from (11) on the boundaries and in small regions around the leading edge and trailing edge. The rest of the field was filled in by squaring.

The value of r from (7) was $r = 1{\cdot}0111$. Taking the chord $c = 0{\cdot}5044$ we obtain the channel half width $h = 0{\cdot}5715$.

The mean blockage as obtained from $1 + \varepsilon \simeq r$ is $\varepsilon \simeq 0{\cdot}0111$. This can be compared with the usual value[2].

$$\varepsilon = (1 + t/c)\frac{\pi}{6}\frac{A}{H^2} = 0{\cdot}0113\,. \qquad (13)$$

Fig. 3 shows the blockage factor ε along the aerofoil and along the channel wall (*see* also Table 6). Contours of ε are shown in Fig. 2 and contours of velocity in Fig. 4. Table 3 gives the free-stream velocity and the increment in velocity due to the channel walls throughout the main part of the field.

3.2. It is interesting to note in Fig. 3 how the blockage effect rises as the aerofoil is approached along the axis, reaching a maximum behind the position of maximum velocity. The maximum value is 4·5 per cent greater than the mean over the aerofoil. The distribution over the aerofoil would be more uniform if the ratio of channel width to chord were larger as in most practical cases it is. The increase in blockage effect as the wall is approached (Fig. 2) is perfectly normal as can be seen by referring to Ref. 3, Fig. 7.

The total velocity due to the aerofoil and the walls is shown in Fig. 4. The value on the wall opposite the aerofoil centre is 1·0321 (Table 3).

It has been shown by Thom and Jones (Ref. 6) that the ratio of the maximum incremental velocity at the aerofoil produced by the walls to that on the walls produced by the aerofoil is

$$R = \frac{1}{3} + \frac{4\pi^2}{15}\frac{K^2}{H^2} \qquad (14)$$

where K is the radius of gyration of the aerofoil profile about an axis through the centroid at right-angles to the chord. In our example we have

$$K/c = 0{\cdot}237 \qquad H/c = 2{\cdot}27 \quad \text{so that from (14)}$$
$$R = 0{\cdot}362.$$

To compare with this we have the following values calculated from the fields

Mean velocity over aerofoil (open channel)	1·12
Mean velocity over aerofoil (with walls)	1·12 × 1·0111
Incremental velocity on walls (Table 3)	0·0321

These give $R = 0{\cdot}39$.

If we use the maximum increment in velocity on the aerofoil we find a larger value of R namely 0·43.

3.3. It is believed that the above is a fairly accurate arithmetical study of the tunnel-wall effect on a symmetrical aerofoil at zero incidence. The grid was 10 squares to the chord but as we were operating on the difference of two fields no serious error is likely to have been thereby introduced.

4. *Compressible Flow.*—For the compressible flow it was considered desirable to develop a method depending on the use of the velocity vector which could possibly be adapted to cover cases where a shock wave was present in the field. The method is shown to be capable of dealing with the supersonic region but a discussion of shock waves is not included. It is proposed to operate on the 'grid' given by the orthogonal network obtained from the incompressible solution given in the preceding sections.

4.1. *Theory of the Compressible Solution.*—Let the velocity vector for the incompressible case be q_1, θ_1 and for the compressible case q, θ.

We wish first to obtain suitable expressions for $\nabla^2 \log 1/q$ and $\nabla^2\theta$ since these are zero for the incompressible case.

Take the fundamentals in the form:

Bernoulli

$$\left.\begin{aligned} \frac{1}{2}\frac{\partial q^2}{\partial x}+\frac{1}{\rho}\frac{\partial p}{\partial x}-\zeta v=0 \\ \frac{1}{2}\frac{\partial q^2}{\partial y}+\frac{1}{\rho}\frac{\partial p}{\partial y}+\zeta u=0 \end{aligned}\right\} \quad (15)$$

Continuity

$$\frac{\partial(\rho u)}{\partial x}+\frac{\partial(\rho v)}{\partial y}=0 \quad (16)$$

Vorticity

$$\frac{\partial v}{\partial x}-\frac{\partial u}{\partial y}=\zeta \quad (17)$$

Putting $a^2=\partial p/\partial\rho$, where a = velocity of sound, Bernoulli's equation can be written

and

$$\left.\begin{aligned} \frac{1}{2a^2}\frac{\partial q^2}{\partial x}+\frac{1}{\rho}\frac{\partial \rho}{\partial x}-\frac{\zeta v}{a^2}=0 \\ \frac{1}{2a^2}\frac{\partial q^2}{\partial y}+\frac{1}{\rho}\frac{\partial \rho}{\partial y}+\frac{\zeta u}{a^2}=0 \end{aligned}\right\} \quad (18)$$

Using these, the continuity equations can be written

$$\frac{\partial u}{\partial x}+\frac{\partial v}{\partial y}=\frac{1}{2a^2}\left(u\frac{\partial q^2}{\partial x}+v\frac{\partial q^2}{\partial y}\right) \quad (19)$$

Put $u=q\cos\theta$, $v=q\sin\theta$, $A=\frac{\partial q}{\partial x}+q\frac{\partial\theta}{\partial y}$, $B=\frac{\partial q}{\partial y}-q\frac{\partial\theta}{\partial x}$

and

$$\lambda_0=\left(\frac{\partial q^2}{\partial x}\cos\theta+\frac{\partial q^2}{\partial y}\sin\theta\right)\frac{1}{2a^2} \quad (20)$$

Then (19) can be written

$$A\cos\theta+B\sin\theta=q\lambda_0 \quad (21)$$

Similarly (17) can be written

$$A\sin\theta-B\cos\theta=\zeta \quad (22)$$

Solving these for A and B and noting that

$$\frac{\partial}{\partial y}\log\frac{1}{q}=-\frac{1}{q}\frac{\partial q}{\partial y} \qquad \text{we find}$$

and

$$\left.\begin{aligned} -\frac{\partial\theta}{\partial x}-\frac{\partial}{\partial y}\log\frac{1}{q}=\lambda_0\sin\theta-\frac{\zeta}{q}\cos\theta \\ \frac{\partial\theta}{\partial y}-\frac{\partial}{\partial x}\log\frac{1}{q}=\lambda_0\cos\theta+\frac{\zeta}{q}\sin\theta \end{aligned}\right\} \quad (23)$$

Differentiating and combining we obtain

$$\left.\begin{aligned} \nabla_z^2\theta=-\frac{\partial}{\partial x}\left(\lambda_0\sin\theta-\frac{\zeta}{q}\cos\theta\right)+\frac{\partial}{\partial y}\left(\lambda_0\cos\theta+\frac{\zeta}{q}\sin\theta\right) \\ \nabla_z^2\log\frac{1}{q}=-\frac{\partial}{\partial x}\left(\lambda_0\cos\theta+\frac{\zeta}{q}\sin\theta\right)-\frac{\partial}{\partial y}\left(\lambda_0\sin\theta-\frac{\zeta}{q}\cos\theta\right) \end{aligned}\right\} \quad (24)$$

It would probably be possible to use these for squaring θ and $\log 1/q$ but it is better to transform to the w field which is given by the Laplacean solution already obtained for the field having the same boundaries. We have

$$w = \phi + i\psi, \qquad q_1^2 = \left(\frac{\partial\phi}{\partial x}\right)^2 + \left(\frac{\partial\phi}{\partial y}\right)^2.$$

Further let θ_1 be the angle between the x-axis and the incompressible velocity vector; and let α be the angle between the incompressible and the compressible vectors.

Thus $\theta = \theta_1 + \alpha$.

Then we get

$$\left.\begin{aligned} \nabla_w^2\theta &= -\frac{\partial}{\partial\phi}\left(\lambda\sin\alpha - \frac{\zeta}{qq_1}\cos\alpha\right) + \frac{\partial}{\partial\psi}\left(\lambda\cos\alpha + \frac{\zeta}{qq_1}\sin\alpha\right) \\ \nabla_w^2\log\frac{1}{q} &= -\frac{\partial}{\partial\phi}\left(\lambda\cos\alpha + \frac{\zeta}{qq_1}\sin\alpha\right) - \frac{\partial}{\partial\psi}\left(\lambda\sin\alpha - \frac{\zeta}{qq_1}\cos\alpha\right) \end{aligned}\right\} \quad .. \quad (25)$$

$$\text{where} \quad \lambda = \frac{1}{2a^2}\left(\frac{\partial q^2}{\partial\phi}\cos\alpha + \frac{\partial q^2}{\partial\psi}\sin\alpha\right).$$

Again these could be used as working formulae but the real simplification of the method is obtained by operating on α instead of θ. Thus note that $\nabla_w^2\theta_1 = 0$ and $\nabla_w^2\log 1/q_1 = 0$. Subtract these from (24) and so obtain the final forms.

$$\left.\begin{aligned} \nabla_w^2\alpha &= -\frac{\partial}{\partial\phi}\left(\lambda\sin\alpha - \frac{\zeta}{qq_1}\cos\alpha\right) + \frac{\partial}{\partial\psi}\left(\lambda\cos\alpha + \frac{\zeta}{qq_1}\sin\alpha\right) \\ \nabla_w^2\log q_1/q &= -\frac{\partial}{\partial\phi}\left(\lambda\cos\alpha + \frac{\zeta}{qq_1}\sin\alpha\right) - \frac{\partial}{\partial\psi}\left(\lambda\sin\alpha - \frac{\zeta}{qq_1}\cos\alpha\right) \end{aligned}\right\} \quad .. \quad (26)$$

$$\lambda = \frac{1}{2a^2}\left(\frac{\partial q^2}{\partial\phi}\cos\alpha + \frac{\partial q^2}{\partial\psi}\sin\alpha\right)$$

$$\frac{1}{2a^2} = \frac{M^2}{2U^2\left\{1 - \frac{1}{5}M^2\left(\frac{q^2}{U^2} - 1\right)\right\}} \quad .. \quad .. \quad .. \quad .. \quad .. \quad .. \quad (27)$$

M and U being the free-stream values.

In practice considerable simplification takes place. Except behind shock waves ζ is zero. It is evident that α will in general be a very small angle being simply the change in direction of the streamlines due to compressibility. Thus the terms containing $\sin\alpha$ are negligible over a great part of the field.

5. *A Compressible Solution at* $M = 0{\cdot}7$.—The method described in the last section was applied to the aerofoil used previously in section 3.

Neglecting in first approximation the terms containing $\sin\alpha$ we have

$$\lambda = \frac{1}{2a^2}\frac{\partial q^2}{\partial\phi}$$

and

$$\nabla_w^2\alpha = \frac{\partial\lambda}{\partial\psi}.$$

For a start a first set of λ values was obtained from the incompressible velocity values.

Having settled the α-field we obtain the values for $\log q_1/q$ from

$$\left.\begin{aligned} \frac{\partial}{\partial\psi}\left(\log\frac{q_1}{q}\right) &= -\frac{\partial\alpha}{\partial\phi} - \lambda\sin\alpha \\ \frac{\partial}{\partial\phi}\left(\log\frac{q_1}{q}\right) &= \frac{\partial\alpha}{\partial\psi} - \lambda\cos\alpha \end{aligned}\right\} \quad \ldots\ \ldots\ \ldots\ \ldots\ \ldots\ \ldots \quad (28)$$

which become

$$\log\frac{q_1}{q} = \int_\infty^\phi\left(\frac{\partial\alpha}{\partial\psi} - \lambda\cos\alpha\right)d\phi \text{ along constant } \psi\text{-lines}$$

and $$\log\frac{q_1}{q} = \int_\infty^\psi\left(-\frac{\partial\alpha}{\partial\phi} - \lambda\sin\alpha\right)d\psi \text{ along constant } \phi\text{-lines} . \quad \ldots\ \ldots\ \ldots\ \ldots \quad (29)$$

To avoid any possible trouble at the stagnation points the integrations were done along the top boundary and down each equipotential. With the new values for q another set of values was calculated. As the values for q go up, the first neglected parts have to be taken into account near the aerofoil, so that we now use the full expressions for λ and $\nabla^2\alpha$ given at (26) and (27).

The process was found to converge fairly quickly to the solution shown in Fig. 5. It can be seen that a small supersonic region has developed at this Mach number, but this presented no difficulties.

Fig. 6 shows the pressure coefficient along the aerofoil as calculated from

$$C_p = \frac{10}{7M^2}\left[\left(\frac{5+M^2}{5+M_L{}^2}\right)^{7/2} - 1\right] \qquad \text{for compressible flow}$$

and $$C_p = 1 - q_1{}^2 \qquad \text{for incompressible flow.}$$

Due to the coarseness of the grid used (10 squares to the chord) the curves shown are uncertain in the neighbourhood of the stagnation points but this is investigated in section 6.

To obtain a comparison with the linear perturbation theory we apply the theorem enunciated by Goldstein and Young[8] namely:—'for compressible flow in a tunnel of breadth $2h$ the increase in the longitudinal velocity is $1/\beta$ times the increase in the longitudinal velocity in incompressible flow in a tunnel of breadth $2\beta h$'.

We have from section 3 the incompressible velocity in the unbounded case and in a channel of width H. To obtain the velocities in a channel of width βH we write by analogy with the usual blockage expression*

$$\varepsilon_H = (q_B - q_O)/q_O = Ktc/H^2$$

where q_B and q_O refer to the velocities in the bounded and unbounded cases. It is thus possible to calculate K for each point on the aerofoil. Then we assume that the same value of K applies to the narrow channel so that

$$\varepsilon_{\beta H} = Ktc/\beta^2H^2 .$$

The velocity in the narrower tunnel is then

$$q_{\beta H} = q_O(1 + \varepsilon\beta_H) .$$

Thus, applying the rule given above, the compressible velocity is

$$q = 1 + (q_{\beta H} - 1)/\beta \ldots \quad \ldots\ \ldots\ \ldots\ \ldots\ \ldots \quad (30)$$

* When the blockage effect is only a few per cent it is immaterial whether we use this form or

$$\varepsilon = (q_O - q_B)/U$$

where U is the velocity far upstream, but care has to be taken as to which form is used when the effect becomes so large as it does in this paper in the compressible case.

These values are compared in Fig. 7 with the velocities from the arithmetical solution. It is seen that in the region of high velocity the linear perturbation theory gives too low a value. Things would be improved if instead of using $1/\beta$ in (30) we used the Krámán-Tsien factor but it seems that a still larger factor is necessary to give agreement.

6. *Check Calculation with Finer Grid.*—The process described in the preceding sections has been repeated for the same aerofoil between walls with the same spacing but the work was done on a finer grid; 20 squares to the chord.

6.1. The comparison of the two sets of results is given in Table 4 and shown in Fig. 8. The agreement is seen to be good except that near the leading edge (at $\phi = 1.6$) the coarse grid velocity is slightly lower.

The table also contains the ordinates of the profile at all the grid points.

7. *Open Field Compressible Flow.*—To obtain the tunnel-wall effect it is necessary to have the solution for the same aerofoil in an unbounded stream. This solution was obtained (as in section 3) by operating on the difference in direction between the compressible and incompressible flows. It is shown in section 6.1 that there is no great gain in accuracy by using 20 squares to the chord as against 10. So, as we are interested in the difference between the bounded and unbounded cases, it is sufficient to use 10 squares.

It has been shown by Woods (Ref. 11, Part N) that

$$q\,(\phi, \psi) = [q_1(\phi, \beta\psi)]^{1/\beta} \quad \ldots\ldots\ldots\ldots\ldots\ldots\ldots\ldots \quad (31)$$

and

$$\theta\,(\phi, \psi) = \theta_1(\phi, \beta\psi) \quad \ldots\ldots\ldots\ldots\ldots\ldots\ldots\ldots \quad (32)$$

where q, θ refer to the compressible flow and q_1, θ_1 to the incompressible. (31) and (32) were used to start the solution. An outer boundary was taken at $\psi = 4$ or roughly one chord distant from the aerofoil. The values of $\alpha \equiv \theta - \theta_1$ were calculated along this boundary by making use of (32). In brief, this reduces to using

$$\alpha = \int_4^{2.857} \frac{\partial \log 1/q}{\partial \phi}\, d\psi \text{ where } 2.857 \equiv 4\beta$$

to find the boundary values. The assumption is that (32) is likely to be a good approximation at points well back from the aerofoil and that any residual error there will not seriously affect the values on the surface obtained by squaring from $\psi = 4$ to the aerofoil.

Two complete rounds were worked on the field; from these the values of q in Table 5 were obtained. It will be seen that the values are still altering slightly after the 2nd round. Final values obtained by extrapolation are shown in Table 6. The method of extrapolation used has already been described in Ref. 1, §9. Table 6 also contains blockage factors deduced by a comparison with the bounded case in Table 4. The blockage for the incompressible case is given for comparison.

The velocity distribution on the aerofoil surface is compared with the incompressible and with the linear perturbation theory value in Fig. 9.

8. *Compressible Blockage.*—Fig. 10 compares the compressible and incompressible blockage factors and Fig. 11 shows their ratio. On the linear perturbation theory the ratio is $1/\beta^3$ or 2·75. It is seen that in the region of maximum thickness the blockage factor is much higher than towards the ends. In Ref. 10 Woods shows that the blockage effect is a maximum near the centroid of the section.

8.1. *Comparison with Mass Flow Theory.*—In Ref. 9 it is shown that on certain assumptions the blockage factor is given by

$$\varepsilon = 0{\cdot}5\,\frac{tc}{H^2\beta^3} + 0{\cdot}3\,\frac{t^2}{Hc\beta^5}.$$

Replacing the first term by its more usual value and substituting $M = 0.7$, $t/c = 0.147$, $H/c = 2{\cdot}27$, $A/c^2 = 0{\cdot}102$ we get

$$\varepsilon = \frac{\pi}{6}\frac{A}{H^2\beta^3} + 0{\cdot}3\frac{t^2}{Hc\beta^5}$$
$$= 0{\cdot}029 + 0{\cdot}015 = 0{\cdot}044\,.$$

Even this value is not so high as the peak in Fig. 10 but it happens to be not much different from the mean taken over the chord, namely $0{\cdot}046$.

Conclusions.—In sections 2 and 3, a method of finding the incompressible flow past an aerofoil in a channel is developed and used. In sections 4 and 5, a method is given and used of solving the compressible case of the same problem. The advantage of this method is that, as we work directly on the difference in the velocity vector brought about by compressibility, a fairly accurate solution can be achieved, even if the grid is somewhat coarse.

The actual example worked is that of an aerofoil $14\frac{1}{2}$ per cent thick between walls $2{\cdot}27$ chords apart. For these values we draw the following conclusions:

(*a*) The effect of the walls is to raise the surface velocity on the aerofoil rather more towards the centre than at its ends; the maximum occurring about $0{\cdot}45c$.

(*b*) The effect of compressibility alone is to raise the velocity much more in the region of maximum thickness than elsewhere, the maximum change occurring about $0{\cdot}26c$.

(*c*) The effect of walls *and* compressibility is to raise the velocity most at an intermediate position, namely near $0{\cdot}29c$.

(*d*) The mean value of the blockage effect over the chord is roughly 50 per cent higher than that given by the usual image theory combined with the linear perturbation theory. The maximum value being some 70 per cent greater than the mean shows that for an aerofoil of this size, relative to the channel, no single blockage factor can give a representation of velocity over the whole surface.

Physically it would be necessary to use a thinner aerofoil in a wind tunnel to give a proper representation of the velocity distribution on an aerofoil in free air. It should, however, be remembered that the example chosen is an extreme case. Normally such a large aerofoil would not be used in a wind tunnel.

LIST OF SYMBOLS

ϕ, ψ		Velocity potential and stream function, incompressible flow
q_1, θ_1		Velocity vector, incompressible flow
q_O, θ_O, etc.		Refer to the unbounded or open field
q_B, θ_B, etc.		Refer to the flow between walls
H	=	$2h$, Distance between walls
A		Area of aerofoil profile
c		Chord of aerofoil
t		Thickness of aerofoil
λ_O		Defined by equation (20)
λ		Defined by equation (25)
α		$\theta - \theta_1$, Rotation of streamline due to compressibility
r		*See* equation (7)
U		Undisturbed velocity

REFERENCES

No.	*Author*	*Title, etc.*
1	A. Thom	The method of influence factors in arithmetical solutions of certain field problems. R. & M. 2440. August, 1946.
2	J. S. Thompson	Present methods of applying blockage corrections in a closed rectangular high-speed wind tunnel. R.A.E. Report Aero. 2225. A.R.C. 11,385 January, 1948. (Unpublished.)
3	A. Thom	Blockage corrections in a closed high-speed tunnel. R. & M. 2033. November, 1943.
4	N. A. V. Piercy, R. W. Piper and L. G. Whitehead	The new transformed wing sections. *Aircraft Engineering*. November, 1938.
5	N. A. V. Piercy, R. W. Piper and J. H. Preston	*Phil. Mag.* Series 7, Vol. XXIV. 1937. pp. 425 and 1114.
6	A. Thom and Myra Jones ..	Tunnel blockage near the choking condition. R. & M. 2385. August, 1946.
7	A. Thom	Arithmetical solutions of equations of the type $\nabla^4\psi = \text{const.}$ R. & M. 1604. March, 1933.
8	S. Goldstein and A. D. Young	The linear perturbation theory of compressible flow, with applications to wind-tunnel interference. R. & M. 1909. July, 1943.
9	A. Thom	Tunnel wall effect from mass flow considerations. R. & M. 2442. November, 1949.
10	L. C. Woods	A new approach to two-dimensional channel blockage. Communicated by Prof. A. Thom. Oxford University Engineering Laboratory 48. A.R.C. 13,603. December, 1950.
11	L. C. Woods	The two-dimensional subsonic flow of an inviscid fluid about an aerofoil of arbitrary shape. R. & M. 2811. November, 1950.

TABLE 3

Velocities in the Unbounded Field with Increments due to the Walls. Incompressible Flow

ϕ	ψ					
	0	0·8	1·6	2·4	3·2	4
−4	0·9848	0·9870	0·9915	0·9956	0·9984	1·0001
	72	73	73	71	66	58
−3·6	0·9806	0·9843	0·9909	0·9961	0·9993	1·0009
	78	79	79	78	75	68
−3·2	0·9742	0·9810	0·9909	0·9972	1·0005	1·0020
	83	83	86	86	85	80
−2·8	0·9631	0·9774	0·9920	0·9991	1·0021	1·0032
	88	89	92	94	96	94
−2·4	0·9396	0·9757	0·9951	1·0020	1·0042	1·0046
	91	96	99	103	107	94
−2	0(T.E.)	0·9820	1·0011	1·0059	1·0067	1·0062
		100	106	112	120	128
−1·6	0·9906	1·0013	1·0100	1·0107	1·0094	1·0078
	105	108	113	120	131	146
−1·2	1·0497	1·0265	1·0208	1·0161	1·0123	1·0094
	115	115	119	128	141	164
−0·8	1·0901	1·0502	1·0317	1·0212	1·0148	1·0108
	123	121	124	134	150	177
−0·4	1·1219	1·0696	1·0408	1·0254	1·0168	1·0119
	128	125	129	139	158	186
0	1·1483	1·0837	1·0470	1·0280	1·0181	1·0125
	133	128	130	142	161	195
0·4	1·1705	1·0911	1·0490	1·0286	1·0183	1·0126
	135	129	130	142	162	195
0·8	1·1883	1·0891	1·0459	1·0270	1·0174	1·0121
	137	128	130	139	159	191
1·2	1·1996	1·0734	1·0376	1·0232	1·0156	1·0112
	135	123	125	134	153	180
1·6	1·1908	1·0396	1·0253	1·0180	1·0131	1·0098
	130	116	120	129	144	166
2	0(L.E.)	0·9979	1·0121	1·0122	1·0101	1·0082
		107	115	121	134	150
2·4	0·8979	0·9756	1·0014	1·0067	1·0072	1·0066
	92	101	107	114	122	131
2·8	0·9449	0·9728	0·9947	1·0023	1·0045	1·0049
	93	95	100	105	109	113
3·2	0·9640	0·9763	0·9916	0·9992	1·0023	1·0034
	89	90	93	95	98	96
3·6	0·9742	0·9805	0·9906	0·9972	1·0006	1·0021
	84	85	87	87	86	82
4	0·9804	0·9840	0·9907	0·9961	0·9994	1·0011
	79	79	79	79	76	69

TABLE 4

Aerofoil Profile and Comparison of the Surface Velocities from the Coarse and Fine Grid. Bounded case

$M = 0{\cdot}7 \qquad H/c = 2{\cdot}27$

Area of Profile $A = 0{\cdot}101c^2$

Centroid $\bar{x} = 0{\cdot}43c$

	ϕ	x/c	y/c	q_B Coarse grid	q_B Fine grid
Trailing edge	−2	1·00000	0·00000	0	0
	−1·8	0·93726	0·01146		0·9335
	−1·6	0·88018	0·02118	0·998	1·0009
	−1·4	0·82528	0·02728		1·0522
	−1·2	0·77182	0·03769	1·093	1·0948
	−1·0	0·71947	0·04468		1·1335
	−0·8	0·66801	0·05089	1·170	1·1696
	−0·6	0·61730	0·05633		1·2057
	−0·4	0·56724	0·06100	1·238	1·2366
	−0·2	0·51776	0·06487		1·2678
	0	0·46880	0·06792	1·300	1·2981
	+0·2	0·42030	0·07011		1·3302
	0·4	0·37224	0·07138	1·365	1·3638
	0·6	0·32457	0·07164		1·3985
	0·8	0·27727	0·07078	1·423	1·4219
	1·0	0·23031	0·06863		1·4253
	1·2	0·18368	0·06493	1·399	1·4024
	1·4	0·13734	0·05928		1·3542
	1·6	0·09130	0·05086	1·262	1·2836
	1·8	0·04552	0·03769		1·1551
	1·9	0·02273	0·02725		
	1·95	0·01136	0·01947		
Leading edge	+2	0·00000	0·00000	0	0

TABLE 5

Velocities on Aerofoil Surfaces, Open Field

ϕ	Starting q_0	After 1st round	After 2nd round
−2	0	0	0
−1·6	0·9868	0·9740	0·9724
−1·2	1·0702	1·0660	1·0615
−0·8	1·1284	1·1278	1·1278
−0·4	1·1147	1·1786	1·1821
0	1·2136	1·2224	1·2269
+0·4	1·2466	1·2607	1·2679
0·8	1·2734	1·2932	1·3056
1·2	1·2902	1·3047	1·3101
1·6	1·2770	1·2290	1·2258
+2	0	0	0

TABLE 6

Blockage Factor

ϕ	$M = 0{\cdot}7$		$M = 0$	
	q_0	ε	ε_1	$\varepsilon/\varepsilon_1$
−2				
−1·6	0·972	0·027	0·0106	2·5
−1·2	1·061	0·030	0·0109	2·8
−0·8	1·128	0·037	0·0113	3·3
−0·4	1·183	0·047	0·0114	4·1
0	1·230	0·057	0·0115	4·9
+0·4	1·274±0·002	0·072	0·0115	6·3
0·8	1·320±0·005	0·078	0·0115	6·8
1·2	1·313±0·002	0·066	0·0113	5·8
1·6	1·225	0·030	0·0109	2·8
+2·0				

U = velocity at infinity, is unity throughout.

$\varepsilon = (q_B - q_0)/q_0$.

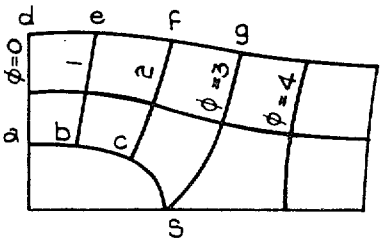

FIG. 1a.

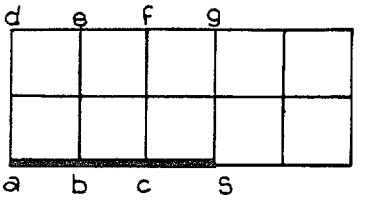

FIG. 1d.

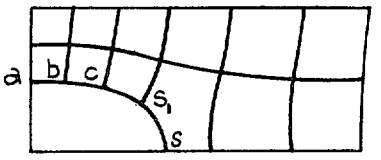

FIG. 1c.

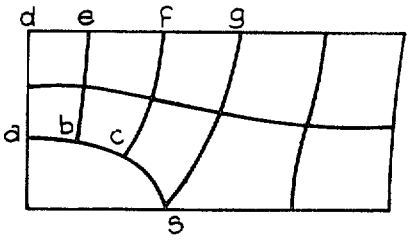

FIG. 1b.

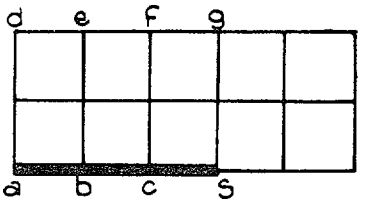

FIG. 1e.

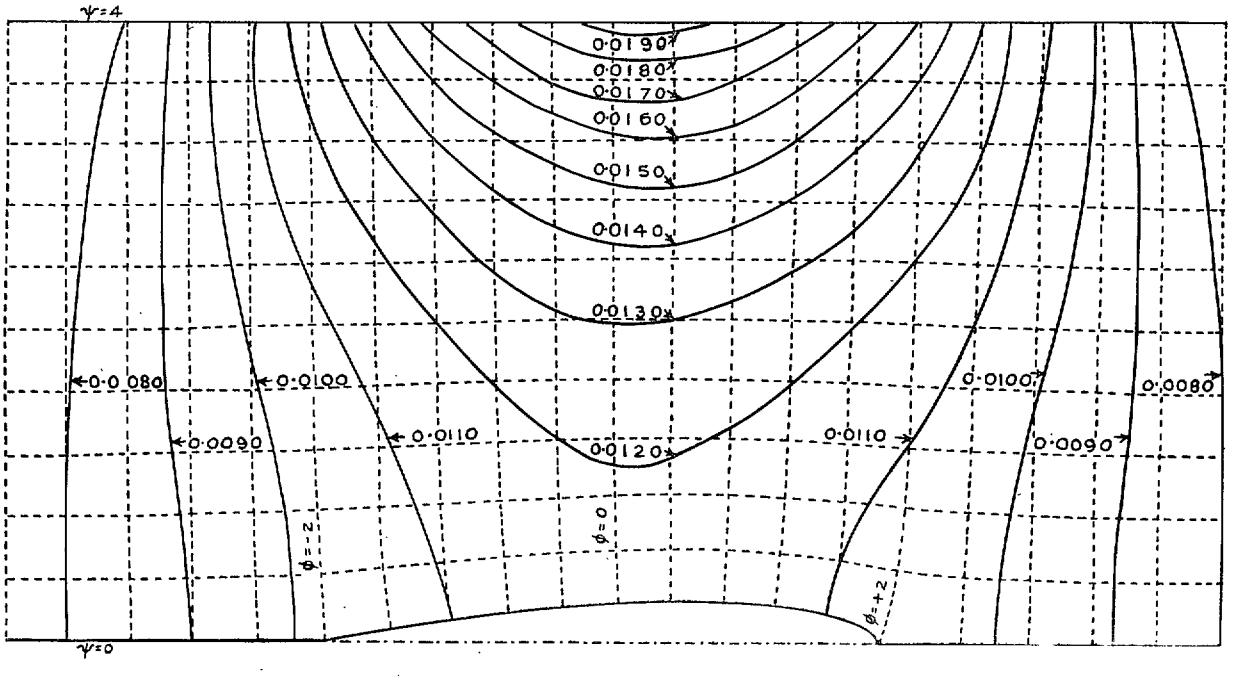

FIG. 2. Contours of blockage factor. $\varepsilon = (q_B - q_0)/q_0$.

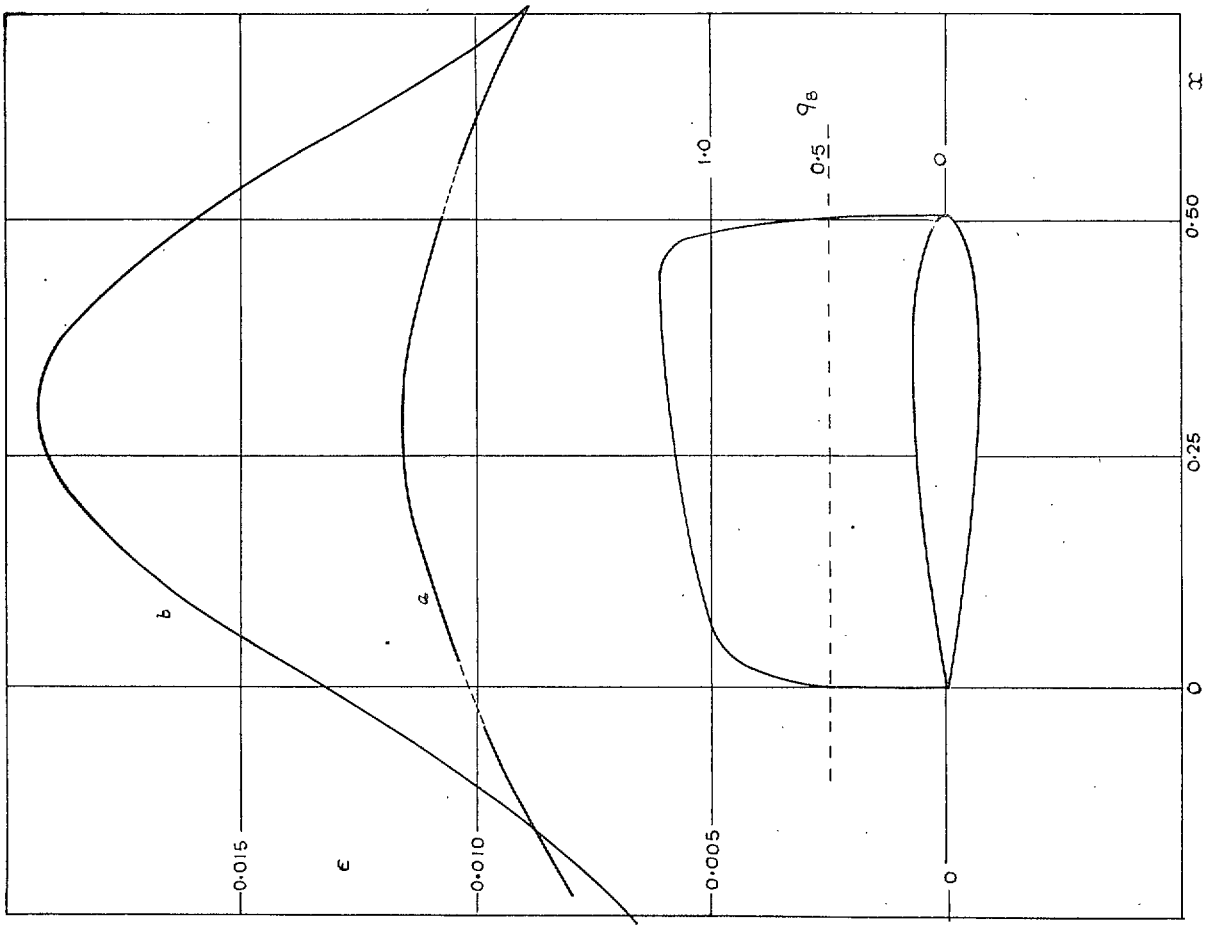

FIG. 3. Blockage factor $\varepsilon = (q_B - q_0)/q_0$ along (a) aerofoil, (b) channel wall, and velocity q_B along aerofoil.

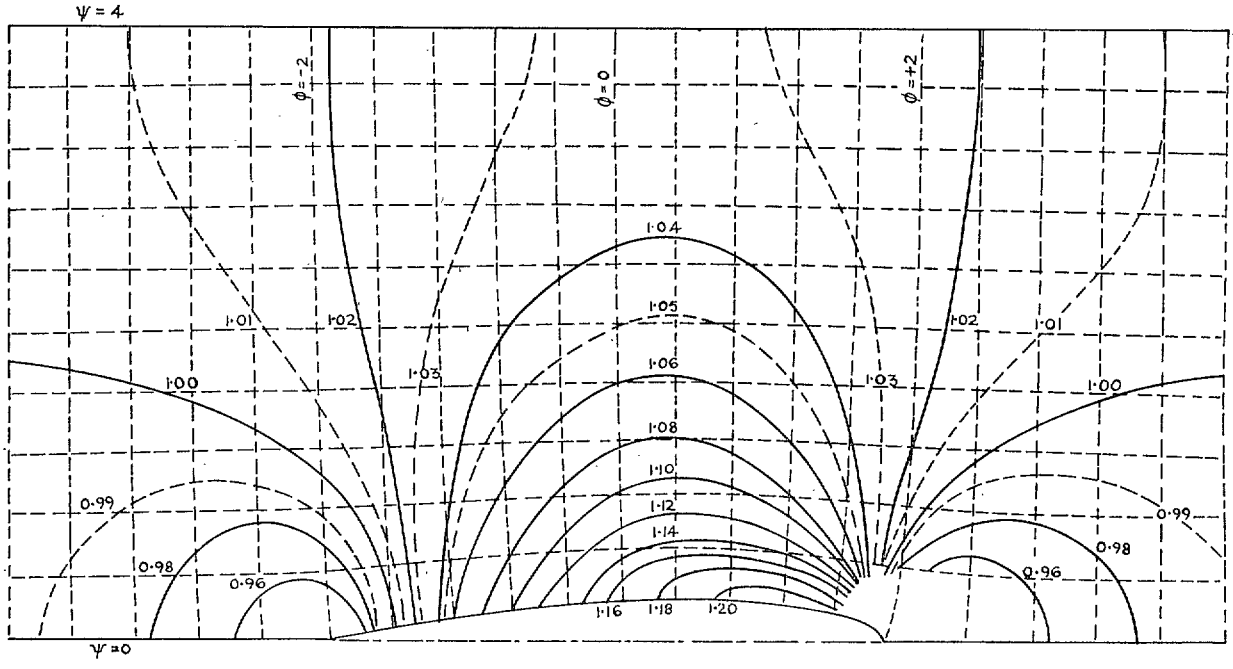

FIG. 4. Contours of velocity q_B in the channel. $U = 1{\cdot}0$.

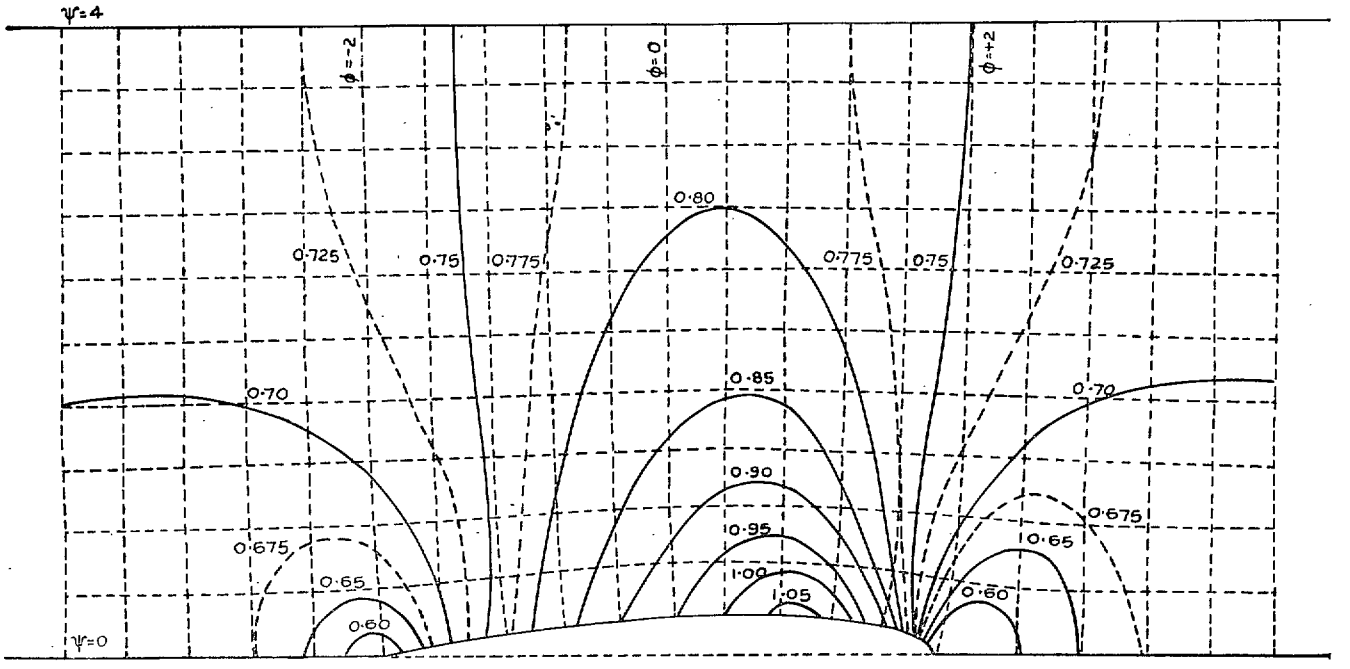

FIG. 5. Contours of local Mach Number. $M = 0{\cdot}70$.

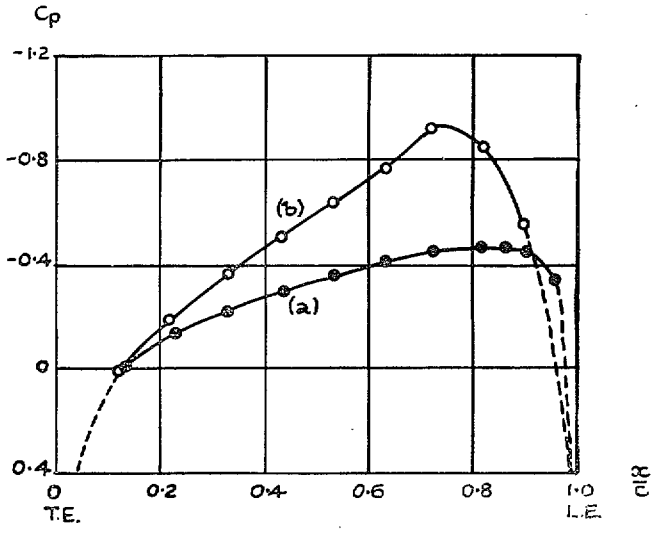

FIG. 6. Pressure distribution along aerofoil. (*a*) incompressible flow, (*b*) compressible flow at $M = 0{\cdot}7$. Overall channel width = 2·27 chords.

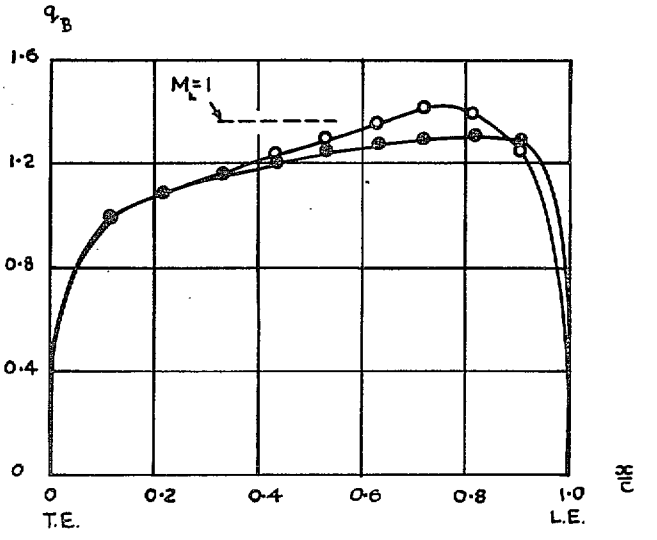

FIG. 7. Velocity distribution along aerofoil at $M = 0{\cdot}7$ ○ squares solution. ● linear perturbation theory. Channel width = 2·27 chords.

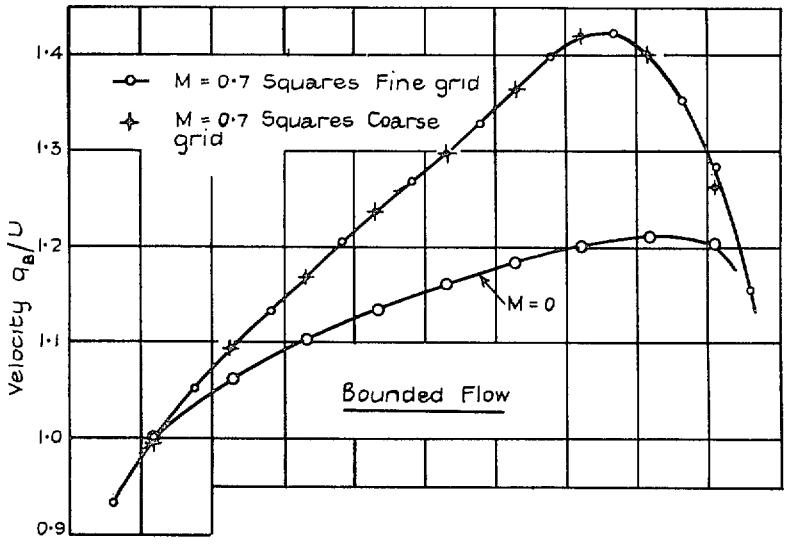

FIG. 8.

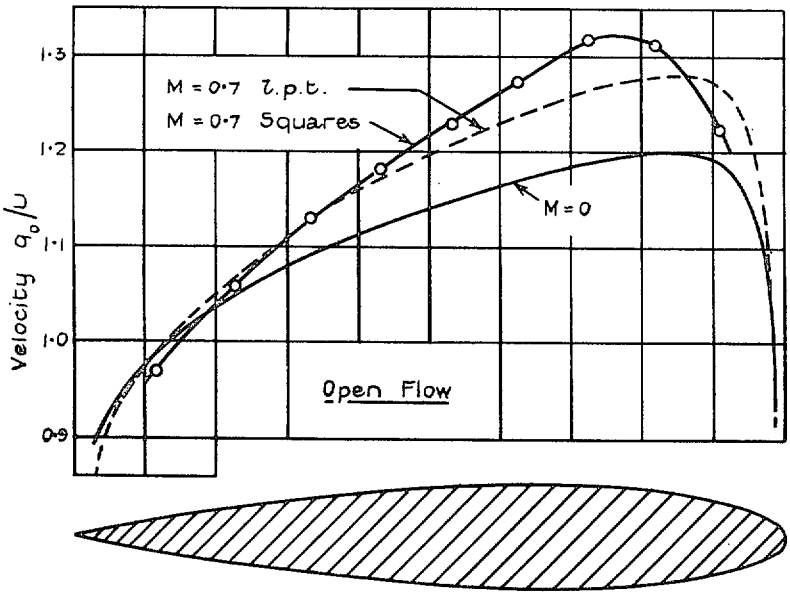

FIG. 9.

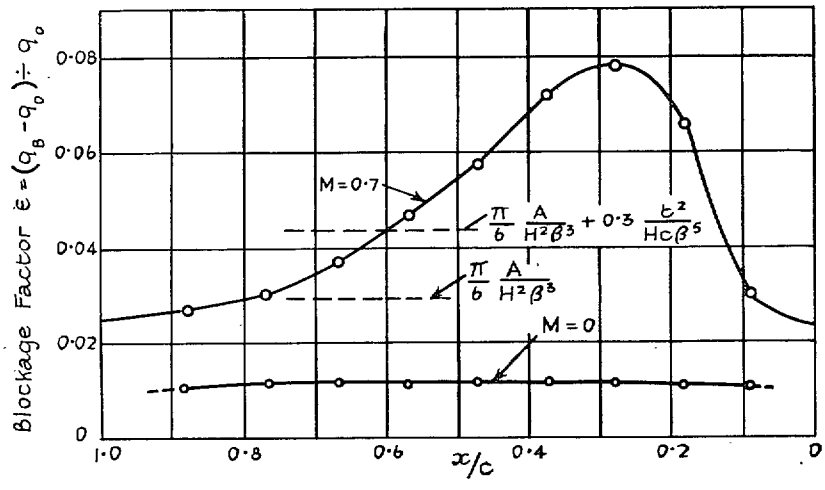

FIG. 10.

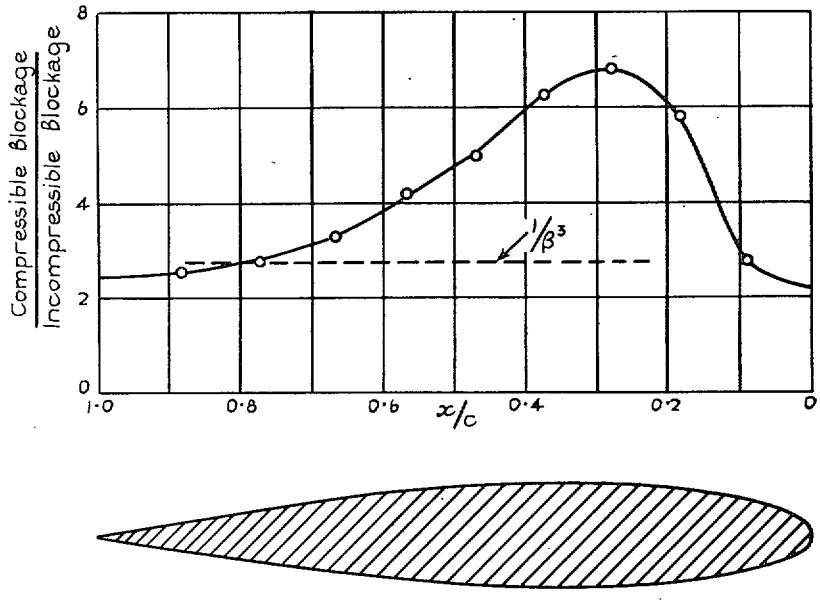

FIG. 11.

Wt. 18/9296 K.7 4/57 G.G. 34-262

PRINTED IN GREAT BRITAIN

Publications of the Aeronautical Research Council

ANNUAL TECHNICAL REPORTS OF THE AERONAUTICAL RESEARCH COUNCIL (BOUND VOLUMES)

1939 Vol. I. Aerodynamics General, Performance, Airscrews, Engines. 50*s.* (51*s.* 9*d.*)
Vol. II. Stability and Control, Flutter and Vibration, Instruments, Structures, Seaplanes, etc. 63*s.* (64*s.* 9*d.*)

1940 Aero and Hydrodynamics, Aerofoils, Airscrews, Engines, Flutter, Icing, Stability and Control, Structures, and a miscellaneous section. 50*s.* (51*s.* 9*d.*)

1941 Aero and Hydrodynamics, Aerofoils, Airscrews, Engines, Flutter, Stability and Control Structures. 63*s.* (64*s.* 9*d.*)

1942 Vol. I. Aero and Hydrodynamics, Aerofoils, Airscrews, Engines. 75*s.* (76*s.* 9*d.*)
Vol. II. Noise, Parachutes, Stability and Control, Structures, Vibration, Wind Tunnels. 47*s.* 6*d.* (49*s.* 3*d.*)

1943 Vol. I. Aerodynamics, Aerofoils, Airscrews. 80*s.* (81*s.* 9*d.*)
Vol. II. Engines, Flutter, Materials, Parachutes, Performance, Stability and Control, Structures. 90*s.* (92*s.* 6*d.*)

1944 Vol. I. Aero and Hydrodynamics, Aerofoils, Aircraft, Airscrews, Controls. 84*s.* (86*s* 3*d.*)
Vol. II. Flutter and Vibration, Materials, Miscellaneous, Navigation, Parachutes, Performance, Plates and Panels, Stability, Structures, Test Equipment, Wind Tunnels. 84*s.* (86*s.* 3*d.*)

1945 Vol. I. Aero and Hydrodynamics, Aerofoils. 130*s.* (132*s.* 6*d.*)
Vol. II. Aircraft, Airscrews, Controls. 130*s.* (132*s.* 6*d.*)
Vol. III. Flutter and Vibration, Instruments, Miscellaneous, Parachutes, Plates and Panels, Propulsion. 130*s.* (132*s.* 3*d.*)
Vol. IV. Stability, Structures, Wind Tunnels, Wind Tunnel Technique. 130*s.* (132*s.* 3*d.*)

Annual Reports of the Aeronautical Research Council—

1937 2*s.* (2*s.* 2*d.*) 1938 1*s.* 6*d.* (1*s.* 8*d.*) 1939–48 3*s.* (3*s.* 3*d.*)

Index to all Reports and Memoranda published in the Annual Technical Reports, and separately—

April, 1950 R. & M. 2600. 2*s.* 6*d.* (2*s.* 8*d.*)

Author Index to all Reports and Memoranda of the Aeronautical Research Council—

1909–January, 1954. R. & M. No. 2570 15*s.* (15*s.* 6*d.*)

Indexes to the Technical Reports of the Aeronautical Research Council—

December 1, 1936 — June 30, 1939.	R. & M. No. 1850.	1*s.* 3*d.* (1*s.* 5*d.*)
July 1, 1939 — June 30, 1945.	R. & M. No. 1950.	1*s.* (1*s.* 2*d.*)
July 1, 1945 — June 30, 1946	R. & M. No. 2050.	1*s.* (1*s.* 2*d.*)
July 1, 1946 — December 31, 1946.	R. & M. No. 2150.	1*s.* 3*d.* (1*s.* 5*d.*)
January 1, 1947 — June 30, 1947.	R. & M. No. 2250.	1*s.* 3*d.* (1*s.* 5*d.*)

Published Reports and Memoranda of the Aeronautical Research Council—

Between Nos. 2251–2349	R. & M. No. 2350.	1*s.* 9*d.* (1*s.* 11*d.*)
Between Nos. 2351–2449	R. & M. No. 2450.	2*s.* (2*s.* 2*d.*)
Between Nos. 2451–2549	R. & M. No. 2550.	2*s.* 6*d.* (2*s.* 8*d.*)
Between Nos. 2551–2649	R. & M. No. 2650.	2*s.* 6*d.* (2*s.* 8*d.*)

Prices in brackets include postage

HER MAJESTY'S STATIONERY OFFICE

York House, Kingsway, London W.C.2; 423 Oxford Street, London W.1 (Post Orders: P.O. Box 569, London S.E.1); 13a Castle Street, Edinburgh 2; 39 King Street, Manchester 2; 2 Edmund Street, Birmingham 3; 109 St. Mary Street, Cardiff; Tower Lane, Bristol 1; 80 Chichester Street, Belfast, or through any bookseller

S.O. Code No. 24-2851